Proceedings of
ASME TURBO EXPO 2002
June 3-6, 2002, Amsterdam, Netherlands

GT-2002-30523

HIGH INTENSITY, LARGE LENGTH-SCALE FREESTREAM TURBULENCE GENERATION IN A TRANSONIC TURBINE CASCADE

A.C. Nix, A.C. Smith, T.E. Diller, W.F. Ng, K.A. Thole
Virginia Polytechnic Institute and State University
Blacksburg, VA 24061

ABSTRACT

Heat transfer predictions in gas turbine engines have focused on cooling techniques and on the effects of various flow phenomena. The effects of wakes, passing shock waves and freestream turbulence have all been of primary interest to researchers. The focus of the work presented in this paper is to develop a turbulence grid capable of generating high intensity, large-scale turbulence for use in experimental heat transfer measurements in a transonic facility. The grid is desired to produce freestream turbulence characteristic of the flow exiting the combustor of advanced gas turbine engines. A number of techniques are discussed in this paper to generate high intensity, large length-scale turbulence for a transonic facility. Ultimately, the passive grid design chosen is capable of producing freestream turbulence with intensity of approximately 10-12% near the entrance of the cascade passages with an integral length-scale of 2 cm.

NOMENCLATURE

c	Blade chord length
d_1	Original grid bar diameter - 2.54 cm (1 in.)
d_2	Modified grid bar diameter- 5.08 cm (2 in.)
D_w	Hot-wire probe diameter (5μm)
E(f)	Energy spectra of streamwise velocity component
f	Frequency
I	Momentum flux ratio ($\rho_j u_j^2/\rho_\infty u_\infty^2$)
k_m	Thermal conductivity of air at mean temperature
M	Mass flux ratio ($\rho_j u_j/\rho_\infty u_\infty$)
Ma	Mach number
Nu'	Nusselt number of hot-wire
P_s	Freestream static pressure
P_t	Freestream total pressure
R_{11}	Autocorrelation of streamwise velocity component
Re	Reynolds number
Re_w	Reynolds number of hot-wire
T	Integral time scale
T_m	Mean temperature ($(T_w+T_s)/2$)
T_s	Freestream static temperature
T_t	Freestream total temperature
T_w	Hot-wire operating temperature
Tu	Turbulence intensity $\left(\frac{u'}{U}\right)$
$\tilde{u}$	Instantaneous velocity $(U+u)$
U	Mean velocity $\left(\frac{1}{T}\int_{t=0}^{T}\tilde{u}dt=\frac{1}{N}\sum_{i=1}^{N}\tilde{u}_i\right)$
u	Fluctuating component of velocity $(\tilde{u}-U)$
u′	RMS of fluctuating velocity $\left(\frac{1}{N}\sum_{i=1}^{N}u_i^2\right)^{1/2}$
V	Hot-wire output voltage

Greek Symbols

κ	Wave number (2πf/U)
Λ_x	Integral length-scale
ρ	Density of air
ρ_m	Density of air at mean temperature
τ	Autocorrelation time
μ_m	Dynamic viscosity of air at mean temperature

INTRODUCTION

The desire for increased engine efficiency in modern gas turbine engines has led to increases in thermal load on high-pressure turbine blading due to high combustor exit temperatures. The flowfield in the turbine section is highly turbulent as a result of combustion dynamics and blade row interactions. Prediction of blade surface temperatures therefore requires researchers to study the effects of unsteady flow phenomena on turbine blade surface heat transfer. These unsteady phenomena include wakes and shock waves due to rotor-stator blade passing and freestream turbulence mainly generated in the combustor. The present research focuses on the effects of combustor exit

freestream turbulence on blade surface heat transfer and film cooling effectiveness.

In order to study the realistic effect turbulence has on heat transfer in an experimentally controlled environment, the turbulence must be generated to model combustor exit turbulence. Several research groups have generated high levels of freestream turbulence using different techniques that were investigated specifically for their applicability in a transonic blow down cascade wind tunnel facility. These techniques can be categorized into mock combustor/jets in crossflow and passive and active grids. The majority of the previous research with high levels of freestream turbulence has been in wind tunnel facilities with relatively low speed flows. These facilities typically concentrate on matching engine representative Reynolds number (Re). The facility for this work is a transonic facility that matches closely with engine Reynolds number, as well as Mach number (Ma). The high velocity, slightly compressible flow at the inlet of the cascade poses a problem in generation of high levels of freestream turbulence.

This paper focuses on the development of a turbulence grid designed to produce high intensity, large length-scale freestream turbulence in high-speed flow. The generator was designed to produce freestream turbulence with a turbulence intensity (Tu) of approximately 15-20% with an integral length scale of 3-4 cm. This desired turbulence level (intensity and scale) was determined by matching results by Van Fossen [1]. He used a 60° section of a GE 90 combustor in a wind tunnel to model the exit flow of a combustor, including inlet swirl vanes, film cooling holes and dilution holes. All three of these combustor components contribute strongly to the combustor exit turbulence conditions. Hot-wire surveys were performed downstream of the combustor section to determine turbulence intensity and length scale. Combustion was not included, but previous research by Moss and Oldfield [2] showed that turbulence intensity and length scale were not significantly affected by the presence of combustion. Van Fossen measured turbulence intensities as high as 20% with length-scales between 1 and 1.5 cm. Using these results, the desired length scale was based on matching the ratio of length scale to blade chord length (Λ_x/c) of the transonic turbine cascade facility to the blades of a GE 90 engine.

In performing this research, a methodical approach was taken. First, grid turbulence was generated to compare with previously reported data under low speed conditions. Second, the grid was tested in the transonic wind tunnel to quantify the turbulence and compare the results with the low speed testing. Third, based on inadequate turbulence results of the initial design, the grid was modified to the current design. Results of measured mean and turbulent quantities will be presented.

REVIEW OF GENERATING TECHNIQUES

Mock Combustor/Jets in Crossflow

Ames [3] designed a mock combustor where air was directed through a liner into the mainstream flow. The main flow is directed along the walls of the liner and two rows of holes were used to simulate dilution injection flows. Turbulence levels of 13% were achieved with an integral length scale of 1.6 cm. The ratio of length scale to true chord length was $\Lambda_x/c=0.11$. A similar combustor simulator, designed by Wang, Goldstein and Olson [4], had a front panel on the inlet to the simulator with four slots and guide vanes on the inside to force a swirling flow along the sidewalls of the simulator. Rows of holes were placed along the sidewalls to simulate cooling flow and dispersion jets. The highest turbulence parameters achieved were a turbulence intensity of 18% and length scale of 8 cm ($\Lambda_x/c=0.43$).

Schauer and Pestian [5] designed a turbulence generator where secondary flow was injected into the mainstream from two opposing rows of holes located upstream of the test section. The jet to freestream velocity ratio was 14. Turbulence parameters achieved were 17% turbulence intensity and length scale was 8 cm [6].

Thole, et al. [7] used small, high velocity normal jets injected into cross flow. A splitter plate was placed between the jets to prevent interaction of the jets. Further improvements using a downstream cylinder were made by Harrington et al. [8] to reduce bulges in the mean flow. The turbulence parameters achieved were up to 20% intensity and 2-3 cm length scale. Later work by Thole led to the design of a large-scale combustor simulator in a low speed, close-loop wind tunnel facility. The combustor simulator, detailed in Barringer et al. [9] produced turbulence intensities of 18% and length scale of 6.5 cm ($\Lambda_x/c=0.11$), using large dilution jets.

Grid or Bar Generators

Mehendale and Han [10] used an active grid made of hollow brass tubes with holes drilled at the grid intersections. Blowing was done uniformly in the co-flow (downstream) direction only, with injection ratio (injection mass flow rate/freestream mass flow rate) of 2.5%. Turbulence intensity of 12.9% was reported, but flow uniformity was reportedly not good.

Sauer and Thole [11] and Radomsky and Thole [12] developed a turbulence generator with simultaneous upstream and downstream blowing from vertical bars. The generator was designed to produce turbulence up to 20% intensity and a range of length-scales by adjusting bar spacing and blowing rates.

Polanka and Bogard [13] developed a turbulence generator which creates turbulence up to 20% in a passive bar arrangement. The generator provided high intensity, large-scale turbulence with good flow uniformity by designing a bar grid with large flow blockage.

Boyle et al. [14] produced turbulence using parallel round bars with relatively large flow blockage and the option of active blowing. Turbulence of greater than 10% was produced with approximately 1.5 cm length scale. It was shown that active blowing significantly improved flow uniformity but reduced overall turbulence. Giel et al. [15] produced turbulence in a transonic facility using an active blowing grid of square bars. The grid incorporated blowing in the upstream direction only at a rate of approximately 5% of the cascade mass flow rate. Blowing air supply pressure to the grid was 125 psig (965 kPa). Turbulence intensity and length scale were 10% and 2.2 cm ($\Lambda_x/c=0.17$), respectively. The work by Giel was of significant interest, since the facility is a transonic tunnel with inlet Mach number similar to the blowdown facility for this study. This was the only other study producing high intensity, large-scale turbulence in a transonic facility.

EXPERIMENTAL APPARATUS AND INSTRUMENTATION

Low Speed Facility

The setup for low speed testing of the grid consisted of a 5 HP blower attached to several transition pieces, followed by a test section. The blower created a mainstream flow velocity of approximately 20 m/s at the entrance to the test section, whereas the inlet velocity of the transonic wind tunnel is approximately 120 m/s. The low speed test setup was designed such that the inlet geometry was identical to the transonic facility from the grid downstream to the test section. The cross-sectional area at the grid location is 38.1 cm (15 in.) by 22.86 cm (9 in.) and is followed by a 2-D contraction to the test section area. A

Plexiglas test section 51 cm (20 in.) in length, 15.2 cm (6 in.) wide and 30.5 cm (12 in.) high was fabricated to take data downstream of the turbulence grid. The cross sectional area of the test section was also designed to match the area of the transonic facility. A flow straightener section was installed in the setup to lower background turbulence levels to less than 2% upstream of the turbulence grid. Blowing air for the turbulence-generating grid was supplied through high-pressure lines to a plenum tank. The plenum supplied air to each of the three blowing bars of the grid.

Transonic Wind Tunnel Facility and Cascade Test Section

The experimental facility in which the turbulence grid was ultimately to be designed for use was a transonic blowdown cascade wind tunnel. Previous research in this facility has been published by Holmberg [16], Nix et al. [17,18], Smith et al. [19] and Popp et al. [20]. The facility allows for run times of up to 35 seconds with the inlet total pressure maintained by a feedback control scheme. The facility is capable of heated runs by way of a heating loop built into the tunnel upstream of the cascade test section. A schematic of the wind tunnel and cascade test section, including the turbulence grid, is shown in Figure 1.

The test section contains a cascade of four full and two half first stage rotor blades forming five passages. The turbine blades are scaled up three times to allow for a film cooling scheme and instrumentation on both surfaces of the blades. The span is 15.3 cm (6 in.) and the aerodynamic chord is 13.7 cm (5.4 in.). The Reynolds number based on aerodynamic chord and exit conditions is about $6 \cdot 10^6$. The inlet Mach number to the cascade test section is approximately 0.4, with unheated flow mainstream velocity of approximately 120 m/s. For ease of installation and removal, the turbulence grid was designed to be placed directly upstream of the 2-D contraction entering the cascade normal to the inlet flow direction. Again, the geometry of the cross-sectional area at the grid location downstream to the test section was identical to the low-speed facility.

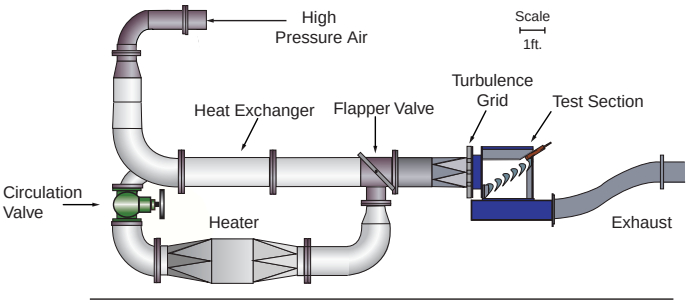

Figure 1. Transonic blowdown facility used for the experiments

Instrumentation

Pressure, temperature and velocity were measured in this study. In the low speed facility, blowing bar plenum pressure and temperature were measured. The bar plenum pressure taps were connected to 0-100 psi pressure transducers. Freestream velocity upstream of the turbulence grid was measured using a pitot-static probe connected to a differential pressure transducer with a range of 2 inches of water. In the transonic facility, freestream total and static pressures were measured using a pitot-static probe, total pressure probe traverse and wall static pressure taps. All pressure taps were connected to 0-15 psi differential pressure transducers. Temperature in the transonic facility was measured using a type K total temperature probe located upstream of the cascade test section. Time-resolved velocity was measured in both the low and high-speed facilities using a hot-wire anemometer. The hot-wire was 5 μm in diameter and approximately 1.5 mm in length. Measurements were performed at an overheat ratio of 1.5. The orientation of the wire was such that the wire was parallel to the span of the turbine blade. Two separate methods, one for each facility, were required to calibrate the hot-wire.

The hot-wire anemometer for low speed testing was calibrated using an air jet calibrator. The hot-wire probe was placed in a low turbulence air jet of known velocity and similar operating temperature as the low speed tunnel. The velocity of the jet was varied and the output voltage of the wire was measured and recorded. The hot-wire voltage vs. velocity data was then fit with a fourth order polynomial. Using this calibration curve, the time-resolved hot-wire voltage measurements performed in the low speed tunnel could be converted to velocity for calculation of turbulent quantities.

Use of the hot-wire probe to measure time resolved velocity in the transonic facility required a separate calibration of the probe. Use of the probe in a compressible flow field does not allow for a simple calibration of voltage versus velocity. To account for compressible flow, the wire was calibrated in-situ in the wind tunnel through a blowdown calibration. The wire was placed in the wind tunnel and the wire output voltage was recorded, along with the tunnel total temperature and total and static pressures from a pitot-static pressure probe located very close to the hot-wire probe. The tunnel was run and the total pressure was allowed to drop to very low values, unchoking the cascade and providing lower Reynolds numbers. The data from these measurements was then used to plot a calibration curve of wire Reynolds number (Re_w) and Nusselt number (Nu'). The data was then curve fit with a power law to give an equation of the type:

$$Nu' = C \cdot \mathrm{Re}_w^x \qquad (1)$$

where the wire Reynolds number and Nusselt number are determined by:

$$\mathrm{Re}_w = \frac{\rho_m \tilde{u} D_w}{\mu} \qquad (2)$$

$$Nu' \propto \frac{V^2}{k_m (T_m - T_s)} \qquad (3)$$

All wire properties were constant given a constant temperature anemometer that maintains wire resistances during the run.

Time-resolved data from the hot-wire during test runs could then be converted from hot-wire voltage to Nusselt number and the wire Reynolds number could be determined with the blowdown calibration curve. All values in Equations (2) and (3) could be measured during a test run, but the product ($\rho_m \tilde{u}$) could not be decoupled since the wire will respond to fluctuations in velocity as well as density. The product of density and velocity ($\rho_m \tilde{u}$) was determined for every hot-wire data point from a measured hot-wired voltage, mean static pressure and static temperature. Since fluctuations in density are small compared to fluctuations in velocity, the instantaneous velocity could be determined by dividing the $\rho_m \tilde{u}$ product by the average flow density determined for the data-sampling period from measurements of static pressure and temperature to yield velocity:

$$\tilde{u} = \rho_m \tilde{u} / \rho \qquad (4)$$

Figure 2 shows a sample blowdown calibration of the hot-wire. Also included in the plot is data taken from a small blowdown wind tunnel

used for calibration of various probes for use in compressible flows. The data from the small wind tunnel spans a larger Reynolds number range than that achievable during blowdown calibration. The data from the two different tunnels are in good agreement.

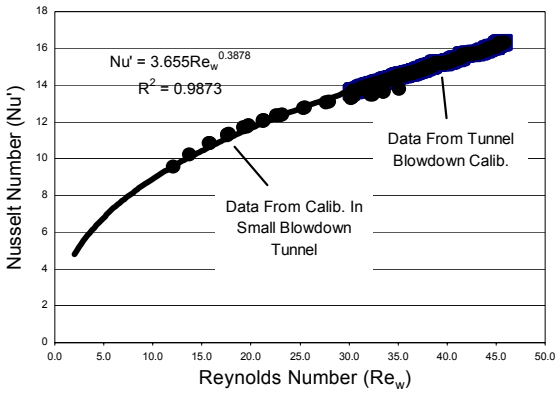

Figure 2. Sample hot-wire blowdown calibration curve

Data Acquisition and Reduction

To characterize the turbulence from the turbulence grid, calibration of the hot-wire was necessary, and statistical and spectral analyses were performed on the time-resolved velocity data. For low speed tests, the data were sampled at 20 kHz, filtered at 10 kHz and a 5V DC offset was applied to increase dynamic resolution. All data points were sampled for 6 seconds and four samples were taken at each point for averaging purposes. For the transonic facility testing, the data was sampled at 100 kHz and filtered at 40 kHz, providing shorter sampling periods of approximately 1.3 seconds. The DC offset was adjusted to account for higher flow velocity to provide better dynamic resolution of the signal.

Statistical and spectral analyses included calculation of the mean velocity (U), fluctuating component of velocity (u), root mean square (RMS) of the fluctuating component of velocity (u'), autocorrelation (R_{11}), probability density functions (PDF), and power spectral density (PSD).

The streamwise instantaneous velocity signal ($\tilde{u}$) can be decomposed into a mean and fluctuating component as follows:

$$\tilde{u} = U + u \qquad (5)$$

where U is the mean velocity and u is the fluctuating component of velocity. The mean, fluctuating component and RMS of the discretized velocity data were calculated according to the equations in the nomenclature section. Using these values, the turbulence intensity (Tu) of the flow at a given point was calculated by:

$$Tu = \frac{u'}{U} \qquad (6)$$

The autocorrelation (R_{11}) of the fluctuating component of velocity (normalized such that R_{11} is equal to 1 at zero lag, τ=0), was calculated by:

$$R_{11}(\tau) = \left(\frac{\overline{u(t) \cdot u(t+\tau)}}{u'^2} \right) = \frac{1}{N} \left(\frac{\sum_{i=1}^{N} u_i \cdot u_{i+j}}{u'^2} \right) \qquad (7)$$

where $\tau = j \cdot \Delta t$

The autocorrelation was used to determine the integral time scale (T) by integrating under the curve to the first zero crossing.

$$T = \int_{t=0}^{\infty} R_{11}(\tau) d\tau = \sum_{i=1}^{N_0} R_{11i} \cdot \Delta\tau \qquad (8)$$

where N_0 is the point of the first zero crossing.

The streamwise integral length scale, which is representative of the largest eddies in the turbulent flowfield, was then determined by invoking Taylor's hypothesis of frozen turbulence:

$$\Lambda_x = \mathrm{U} \cdot T \qquad (9)$$

The power spectral density (PSD) of each data set was determined and frequency averaged to give a cleaner curve by averaging PSD data over a frequency range of Δf=100 Hz. The power spectral density gives an indication of turbulent energy content of the flow at different frequencies, which are inversely proportional to the size of the turbulent eddies in the flow (the wave number, κ, is equal to 2πf/U). The PSD was also used to check for vortex shedding from the bars. The PSD data was normalized and compared to the theoretical Von Kármán spectrum equation [21]:

$$\frac{E(f) \cdot U}{u'^2 \cdot \Lambda_x} = 4 \cdot \left(1 + \left(\frac{8\pi f \cdot \Lambda_x}{3 \cdot U} \right)^2 \right)^{-5/6} \qquad (10)$$

Figure 3 shows an example of measured turbulence data compared to the Von Kármán equation.

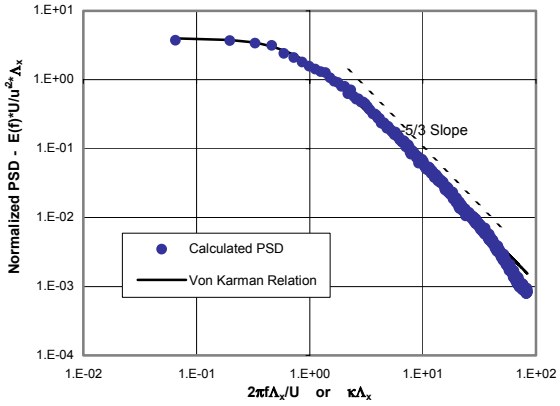

Figure 3. Low speed turbulence PSD compared with Von Kármán equation

Using these statistical and spectral analysis tools, the characteristics of the turbulence could be determined.

Uncertainty Analysis

Precision uncertainty of measurements of velocity was determined using the computerized uncertainty analysis method outlined in Moffat [22]. Uncertainty in the hot-wire velocity measurements in the low speed facility was estimated to be ±1.5%. Uncertainties in turbulence intensity and length scale in the low speed facility were ±2% and ±6%, respectively.

Uncertainty in velocity measurements with the hot-wire in the transonic facility was estimated to be ±2.3%. Uncertainties in turbulence intensity and length scale in the transonic facility were ±3.2% and ±6%, respectively.

LOW SPEED TESTING OF TURBULENCE GRID

As mentioned previously, initial testing of the grid was performed in a low speed wind tunnel. The initial testing served two purposes. First, testing was done to benchmark the turbulence measurement methodology. Second, results were used to obtain baseline numbers to determine what levels of turbulence to expect in the transonic facility and for comparison of turbulence intensity and length scale in two different flow fields.

The initial design of the turbulence grid was based on a combination of results from previous grid generated turbulence work. Simulation of turbulence with a mock combustor or jets in crossflow were not considered, since it was desired to employ a simplistic method. The initial grid design for this work was an actively blown turbulence generating grid incorporating both upstream and downstream blowing. The design was based primarily on work by Radomsky and Thole [12] and by Giel [15]. Both of these studies successfully generated large-scale, high intensity turbulence with actively blown turbulence grids in low and high-speed flow facilities, respectively.

The design that was studied for the present work consisted of three 2.54 cm (1 in.) hollow, square bars spaced 7.62 cm (3 in.) apart between bar edges with no vertical bars. Each bar has nine 3.2mm (1/8 in.) holes spaced 2.54 cm (1 in.) between centers on both the upstream and downstream sides of the bars, allowing for blowing of high-pressure air in both directions. The upstream blowing was performed to increase shear stresses upstream of the grid to produce high turbulence levels. Downstream blowing was performed to fill in the wake areas behind the bars to create better flow uniformity entering the cascade.

Mean and root-mean-square (RMS) velocity measurements were taken at various locations throughout the test section. Flow uniformity was also checked (if wakes are present from bars on grid) in the test section. This traverse was performed at 13 bar widths downstream of the grid. Flow uniformity at this location was shown to be ±2.5%.

Four locations in the streamwise direction downstream of the grid were chosen to take data in the center of the passage (behind the center bar) to calculate the streamwise variation of the turbulence intensity and length scale. These locations are detailed in Table 1.

Table 1: Low Speed Testing Data Acquisition Locations

Location #	Distance Downstream of Grid (x/d)
1	9.5
2	13.5
3	17.5
4	21.5

The mass flow ejected from the grid holes was adjusted in an attempt to reach the turbulence intensity and length scale desired. Momentum flux ratio (I) was believed to be the blowing parameter to match since turbulence is generated from shear stresses, which balance with momentum. Figure 4 - Figure 6 plot the mean velocity, turbulence intensity and length scale versus the blowing rate (as momentum flux ratio). The maximum value of blowing, if plotted as mass flux ratio (M) would be approximately a mass flux ratio of 14. At a momentum flux ratio of 70, the mass flux ratio is approximately 9. The mass flux ratio is, of course, not linear with momentum flux ratio. Of primary importance was the turbulence intensity and length scale, decay of turbulence, flow uniformity and the effect of active blowing. When used in passive mode (i.e. without blowing activated), the grid produced turbulence with intensity of 17% at a distance of 9.5 bar widths downstream of the grid (Location 1), which decayed to approximately 10% at a streamwise distance of 21.5 bar widths (Location 4), with length scales of approximately 2 cm.

The mean flow in the test section without the grid installed was approximately 20 m/s at center passage, which is independent of streamwise measurement location. With the grid installed, Figure 4 demonstrates that at locations near the grid without blowing, there is a velocity deficit due to the wake of the grid bars. This velocity deficit decreases in the streamwise direction and away from the influence of the bars. With blowing activated, the mean velocity in the test section will increase due to addition of mass flow from the blowing bars. Based on holding the inlet velocity fixed, a conservation of mass analysis predicts the expected increase to be from 20 m/s with no blowing to 23 m/s at the highest momentum flux ratio. Another trend that can be seen from the data is the effect of the bar wake. Recall that the measurements shown in Figure 4 are taken directly behind one of the bars (cross-stream surveys were not taken). At low momentum flux ratios there is clearly a reduced velocity at the first position, which is actually most evident at a momentum flux ratio of approximately I=70. Even though there is blowing from the bars at this momentum flux ratio, it is not enough to fill in the bar wakes and yet there is enough upstream blowing to appear as a large blockage for the approaching flow. As a result of this flow blockage, the velocity deficit of the wake appears even greater. At the highest momentum flux ratio the data show there is a fairly constant velocity as the flow progresses downstream, indicating the mean flowfield is likely uniform. The decrease in mean velocity at the highest blowing rate is due to the plenum pressure dropping, most likely due to the inlet flow to the plenum choking.

The turbulence intensity of the flow without the grid installed was approximately 2% upstream of the grid. Figure 5 demonstrates that with the grid in place without blowing, the intensity increases significantly to approximately 10-15% depending on streamwise location. Blowing was used to increase turbulence intensity and create larger length scales. As blowing is activated and increased, there is first a decrease in turbulence intensity, then a steady increase with blowing rate. The initial decrease is due to filling in the wake of the bars, which essentially reduces the effectiveness (or effective bar width) of the grid. This is in agreement with results observed by Boyle [14] where active blowing at low blowing ratios is seen to slightly decrease turbulence intensity.

The integral length scale of the flow was shown, with the exception of one point, to steadily increase with blowing rate as can be seen in Figure 6. The length scale at higher blowing rates is seen to settle out with no further increase. The results show that at approximately 18 bar widths downstream of the grid, the turbulence intensity is as high as 17% with an integral length scale of 3.5 cm. This corresponds to $\Lambda_x/c=0.26$ based on the blade chord length in the transonic facility.

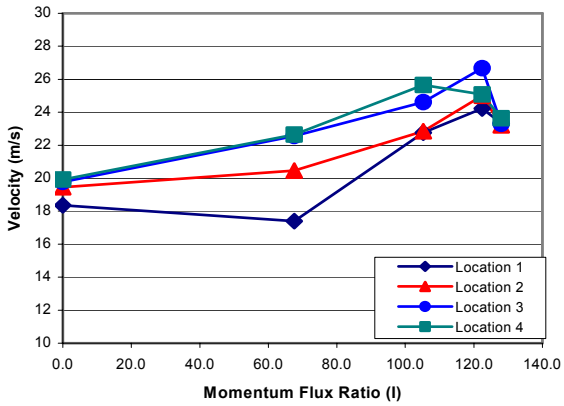

Figure 4. Plot of mean velocity at 4 streamwise locations at different blowing rates

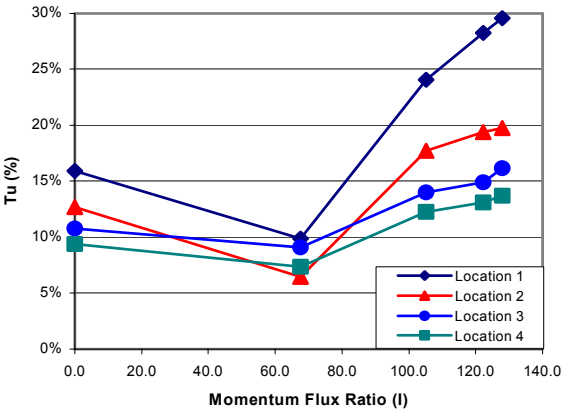

Figure 5. Plot of turbulence intensity at 4 streamwise locations at different blowing rates

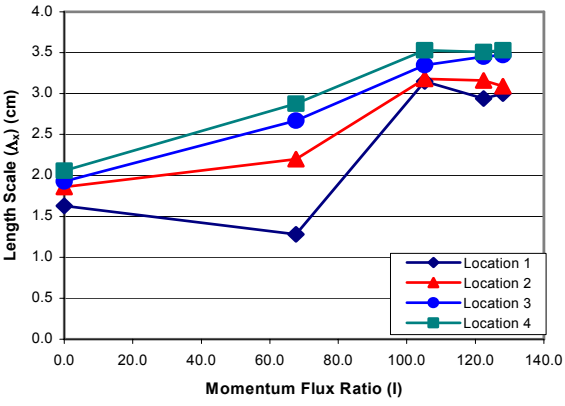

Figure 6. Plot of integral length scale at 4 streamwise locations at different blowing rates

Although the grid only consisted of horizontal bars, which are large compared to the size of the test section, the decay of turbulence intensity without blowing was shown to agree well with published correlations (Baines and Peterson [23]). The decay of turbulence intensity and dispersion of length-scale can be determined by:

$$Tu = c \cdot \left(\frac{x}{d}\right)^{n} \quad \text{and} \quad \Lambda_x = a \cdot d \cdot \left(\frac{x}{d}\right)^{m} \qquad (11)$$

where c and a are constants given as 0.80 and 0.20, respectively, x is the streamwise distance, d is the bar width, and n and m are exponents. The value of n is typically –5/7 and m is between 0.5 and 0.56 according to the published data.

Figure 7 and Figure 8 demonstrate the variation of turbulence intensity and length scale in the streamwise direction, respectively. Results are presented for both the low-speed and high-speed testing of the grid, although the high-speed results will be discussed later in this work. It can be seen in Figure 7 that the low speed turbulence intensity data without blowing agree very well with the published correlations. The decay data with blowing is seen to deviate from this correlation, with greater deviation with higher blowing ratio. Dispersion of length scale does not agree as well with the correlation.

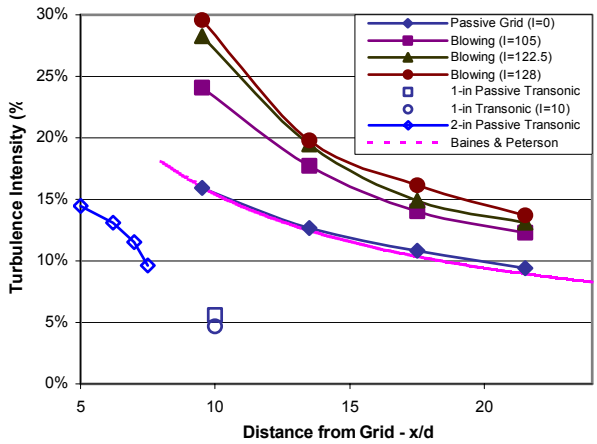

Figure 7. Variation of turbulence intensity in the streamwise direction with and without blowing

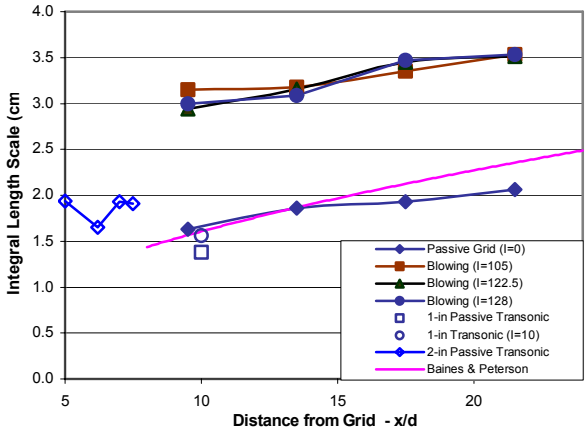

Figure 8. Variation length scale in the streamwise direction with and without blowing

TESTING OF TURBULENCE GRID IN TRANSONIC FACILITY

With initial testing of the grid in the low speed facility providing satisfactory results, the initial grid design was moved to the high-speed facility for testing. Hot-wire data were taken at streamwise locations near those taken in the low speed facility. Data acquisition locations for the transonic facility are illustrated in Figure 9. The locations are shown as T0-T4 to avoid confusion with the locations in the low-speed testing.

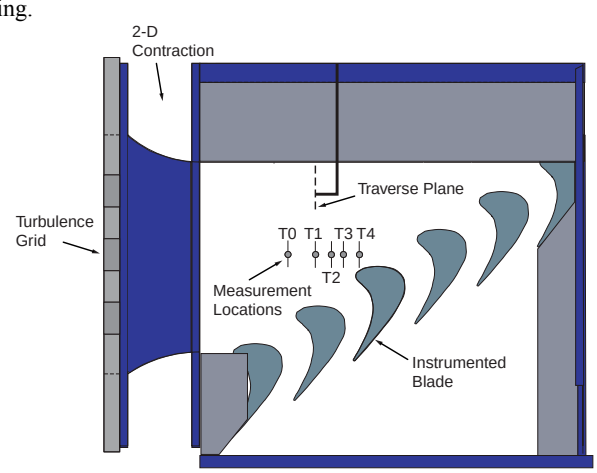

Figure 9. Hot-wire measurement locations in transonic facility

The turbulence grid was initially operated in passive mode in the transonic facility. In passive mode, the turbulence results from the grid did not match the levels measured in the low speed facility, generating test section inlet (location T0) turbulence intensity of only 5% as compared to approximately 12% in the low speed facility, which would decay to even lower levels before reaching the leading edge of the turbine blade cascade. Matching active blowing to the level achieved in the low speed facility was not possible, since matching momentum flux ratio of the blowing would require bar plenum blowing pressures exceeding the levels achievable within the transonic facility. It was determined that blowing pressures approaching 600-700 PSIG would be needed to match bar blowing momentum flux ratio with the low speed tests due to the high velocity and higher density in the freestream. Operating in passive mode (i.e. no blowing), the grid open area was 80% and the bar Reynolds number was much higher than in the low speed test rig (approximately 8 times higher), thus the flow experienced smaller effective blockage and lower turbulence levels when compared to the low speed tests.

In an effort to achieve more desirable turbulence levels in the transonic facility, the turbulence generator was modified by increasing the bar width to 5.08 cm (2 in.) in order to decrease the open area of the grid to 60%. This modification was made based on results achieved by Polanka and Bogard [13] using large bars. This modified grid, operated in passive mode, generated cascade inlet turbulence levels approaching 15%, with an integral length-scale of 2 cm. Blowing was performed with the new grid; however, the turbulence intensity decreased, which is consistent with results reported by Boyle [14]. Blowing at low pressure fills in the wake and thus reduces turbulence intensity. Also, the upstream blowing at low pressure does not generate high turbulence intensity. Again, in order for blowing to have a positive effect on turbulence generation, blowing pressures of higher than what is achievable in the transonic facility are needed.

Measurements of the streamwise decay of turbulence were performed to determine the variation in both turbulence intensity and length scale as the turbulent flow progresses from the inlet of the cascade toward the entrance to the cascade blade passages. These tests were performed with a coarse spacing (only 4 locations) but demonstrated that the turbulence intensity decays to approximately 10-12% approaching the entrance to the cascade passages (location T4). This data is included in Figure 8 and Figure 9. The turbulence decay did not match well with grid generated turbulence decay correlations. The strong decay in turbulence intensity may be due to non-uniform turbulence in the cross-stream direction, or may be a result of effects from the blade (i.e. local velocity is higher due to acceleration of the flow on the suction surface of the blade). Future experiments will be performed to measure cross-stream variation in turbulence intensity and further streamwise decay of turbulence. The length scale of the turbulence does not grow to any extent in the short distance measured, with integral length-scales of approximately 2 cm ($\Lambda_x/c=0.15$) being measured at different streamwise locations. Turbulence parameters for different grid designs (with and without blowing) and measurement locations, including selected data from the low speed testing, are shown in Table 2 below.

Table 2: Turbulence Generation Results

	Location Number	Blowing Rate (I)	Distance from Grid: Original Grid x/d_1	Distance from Grid: Modified Grid x/d_2	Distance from LE of Instr Blade (x/c)	Turbulence Intensity Tu (%)	Length Scale Λ_x (cm)
	2	-	13.5	-	-	13%	2
Low Speed Facility	2	122	13.5	-	-	20%	3.5
Transonic Facility							
1" (2.54 cm) Bars	T0	-	10	-	0.88	5.58%	1.38
	T0	10	10	-	0.88	4.69%	1.56
	T0	-	-	5	0.88	14.45%	1.94
	T1	-	-	6.2	0.47	13.08%	1.65
2" (5.08 cm) Bars	T3	-	-	7	0.14	11.51%	1.93
	T3	10	-	7	0.14	10.62%	2.32
	T4	-	-	7.5	0.05	9.64%	1.91

Total pressure traverse measurements were performed behind the turbulence grid, approximately 10.2 cm (4 in.) upstream of the leading edge of the center cascade passage in order to measure flow uniformity behind the modified grid. Each traverse covered about half the passage in the pitchwise direction. The modified grid has an open area of 60%, with 40% flow blockage area, and thus there was concern with inlet flow non-uniformity due to large bar wakes. Total pressure surveys demonstrate that although there is a significant drop in total pressure across the grid (approximately 7%), the total pressure of the flow approaching the leading edge of the cascade is relatively uniform, with total pressure uniformity of ±1%. The main tunnel flow passes through a 2:1 area contraction downstream of the grid before entering the cascade test section, which is believed to help in merging and mixing of the relatively large bar wakes, thus increasing flow uniformity. Results of the total pressure traverse for both the 2.54 cm (1 in.) and 5.08 cm (2 in.) bar grid designs are shown in Figure 10. It can be seen that the total pressure with the 2.54 cm bars is non-uniform, with wakes present without blowing. With blowing, the total pressure traverse data shows that there is a jet from the bars. The data

for the 5.08 cm bars with blowing shows that there is a smaller total pressure drop across the grid, but the flow uniformity is not greatly improved. Since active blowing actually lowered the turbulence intensity slightly, blowing was not used once the grid was implemented for wind tunnel heat transfer tests.

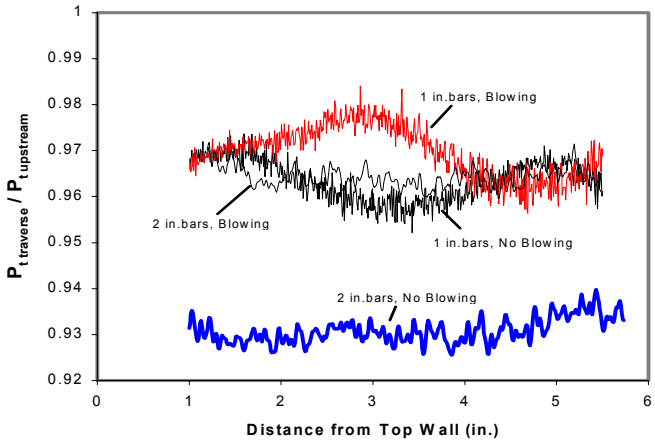

Figure 10. Total pressure uniformity downstream of turbulence grid

CONCLUSIONS

The development of a turbulence generator for use in a high-speed flow facility has been documented. The generator was tested in a low-speed environment with good results in turbulent flowfield and flow uniformity. Results from testing in a high-speed flowfield were in poor agreement with low-speed results due to higher Reynolds number (from higher velocity and density) providing inadequate flow blockage. The momentum flux ratio from low speed testing of the grid could not be matched in transonic facility. The grid was modified to create higher blockage and used as a passive grid. Results from the modified grid showed lower turbulence than originally desired, but with reasonably high intensity (10-12% near the entrance to the cascade passages), large length scale (2 cm) compared to blade chord and good total pressure uniformity downstream of the grid near the entrance to the cascade passages.

ACKNOWLEDGMENT

This work was sponsored by the Air Force Office of Scientific Research (AFOSR), USAF, under grant/contract number F49620-01-1-0177, monitored by Dr. Tom Beutner. We would like to thank Paul Giel, Bob Boyle and Jim Van Fossen at NASA Glenn for their help and insight into developing the turbulence generator.

REFERENCES

[1] Van Fossen, 2000, Personal Communication, NASA Glenn Research Center. Research paper to be published.

[2] Moss, R.W. and Oldfield, M.L.G., 1991, "Measurements of Hot Combustor Turbulence Spectra," ASME 91-GT-351.

[3] Ames, F.E., 1997, "Aspects of Vane Film Cooling with High Turbulence – Parts I and II," ASME 97-GT-239/240.

[4] Wang, H.P., Goldstein, J., and Olson, R.J., 1998, "Effect of High Freestream Turbulence with Large Scale on Blade Heat/Mass Transfer," ASME 98-GT-107.

[5] Schauer, J.J and Pestian, D.J., 1996, "Film Cooling Heat Transfer with High Freestream Turbulence," ASME 96-WA/HT-6.

[6] Bons, J.P., MacArthur, C.A. and Rivir, R.B., 1996, "The Effect of High Free-Stream Turbulence on Film Cooling Effectiveness," ASME *Journal of Turbomachinery*, Vol. **118**, pp. 814-825.

[7] Thole, K.A., Bogard, D.G. and Whan-Tong, J.L., 1994, "Generating High Freestream Turbulence Levels," *Experiments in Fluids* **17**, 375-380.

[8] Harrington, M.K., McWaters, M.A., Bogard, D.G., Lemmon, C.A., and Thole, K.A., 2001, "Full-Coverage Film Cooling with Short Normal Injection Holes," ASME 2001-GT-130.

[9] Barringer, M.D., Richard, O.T., Walter, J.P., Stitzel, S.M., and Thole, K.A., 2001, "Flowfield Simulations of a Gas Turbine Combustor," ASME 2001-GT-0170.

[10] Mehendale, A.B. and Han, J.C., 1992, "Influence of High Mainstream Turbulence on Leading Edge Film Cooling Heat Transfer," ASME *Journal of Turbomachinery*, Vol. **114**, pp. 707-715.

[11] Sauer, J., 1996, "The SUDI Turbulence Generator – A Method to Generate High Freestream Turbulence Levels and a Range of Length Scales," Thesis, University of Wisconsin/Universitat Karlsruhe.

[12] Radomsky, R.W. and Thole K.A., 1998, "Effects of High Freestream Turbulence Levels and Length Scales on Stator Vane Heat Transfer," ASME 98-GT-236.

[13] Polanka, M.D., 1999, "Detailed Film Cooling Effectiveness and Three Component Velocity Field Measurements on a First Stage Turbine Vane Subject to High Freestream Turbulence," Ph.D. Dissertation, The University of Texas at Austin.

[14] Boyle, R. J., Lucci, B.L., Verhoff, V.G., Camperchioli, W.P. and La, H., 1998, "Aerodynamics of a Transitioning Turbine Stator Over a Range of Reynolds Numbers," ASME Paper 98-GT-295 (NASA/TM-1998-208408).

[15] Giel, P.W., Bunker, R.S., Van Fossen, G.J. and Boyle, R.J., 2000, "Heat Transfer Measurements and Predictions on a Power Generation Gas Turbine Blade," ASME 2000-GT-0209.

[16] Holmberg, D.G., 1996, "A Frequency Domain Analysis of Surface Heat Transfer/Freestream Turbulence Interactions in a Transonic Turbine Cascade," Ph.D. Dissertation, Virginia Tech.

[17] Nix, A.C., Diller, T.E. and Ng, W.F., 1997, "Experimental Evaluation of Heat Transfer Effects of Shock Waves on Transonic Turbine Blades," ASME 97-WA/HT-1.

[18] Nix, A.C., Reid, T., Peabody, H., Ng, W.F., Diller, T.E. and Schetz, J.A., 1997, "Effects of Shock Wave Passing on Turbine Blade Heat Transfer in a Transonic Cascade," AIAA-97-0160.

[19] Smith, D.E., Bubb, J.V., Popp, O., Grabowski, H.C., Diller, T.E., Schetz, J.A. and Ng, T.E., 2000, "Investigation of Heat Transfer in a Film Cooled Transonic Turbine Cascade, Part I: Steady Heat Transfer," ASME 2000-GT-202.

[20] Popp, O., Smith, D.E., Bubb, J.V., Grabowski, H.C., Diller, T.E., Schetz, J.A. and Ng, T.E., 2000, "Investigation of Heat Transfer in a Film Cooled Transonic Turbine Cascade, Part II: Unsteady Heat Transfer," ASME 2000-GT-203.

[21] Hinze, J.O., 1975, *Turbulence*, 2nd Edition, McGraw-Hill, New York..

[22] Moffat, R.J., 1988, "Describing Uncertainties in Experimental Results," *Exp. Thermal and Fluid Science* 1988, 1:3-17.

[23] Baines, W.D. and Peterson, E.G., 1951, "An Investigation of Flow Through Screens," *Trans. of the ASME*, July 1951, pp. 467-480.